J Stat Phys (2011) 143: 215–225
DOI 10.1007/s10955-011-0180-4

Dilatancy Transition in a Granular Model

David Aristoff · Charles Radin

Received: 3 November 2010 / Accepted: 13 March 2011 / Published online: 25 March 2011

Abstract We introduce a model of granular matter and use a volume/strain ensemble to analyze infinitesimal shearing. Monte Carlo simulation suggests the model exhibits a second order phase transition associated with the onset of dilatancy.

Keywords Granular matter · Dilatancy · Phase transition

1 Introduction

Static granular matter, such as a sand pile, can exist in a range of densities. In its densely packed state it expands under shear, while when loosely packed it contracts under shear [1]; the boundary between these regimes, 'dilatancy onset', was first popularized by Reynolds in 1885 [2]. We introduce a model in which the transition between these different volume responses to shear appears to be singular, in the precise traditional sense of a second order phase transition, as discussed below. (For two dimensional treatments of the transition see [3–5], and for an interpretation as a glass transition see [6].)

Such modeling can only apply to granular materials in states which are sufficiently reproducible to qualify for the term 'phase'; see [7, 8] for experimental efforts. To determine experimentally whether the response to shear corresponds to a change of phase, the states before and after shear should represent true phases. This necessitates that the shear be infinitesimal, so that it does not drive the material into a more complicated ('nonequilibrium') state. We are mainly concerned, therefore, with modeling the volume reaction to the infinitesimal shear of granular matter. Although, as noted above, the phenomenon of dilatancy onset has been known for over a hundred years, we know of no volume response measurements from which one may directly determine whether or not dilatancy onset is a phase transition. In large part this is due to the difficulty of working with granular samples, in the appropriate range of volume fractions, in states which are sufficiently reproducible [7, 8].

D. Aristoff · C. Radin (✉)
Mathematics Department, University of Texas, Austin, TX 78712, USA
e-mail: radin@math.utexas.edu

Fig. 1 Layers of parallel cubes

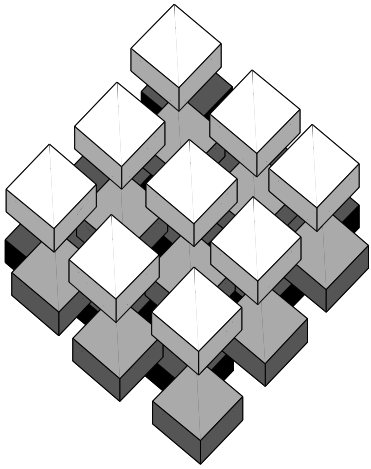

Our modeling follows in a long line of research, championed by Edwards [9], de Gennes [10] and others, in which certain nonequilibrium materials, in particular granular matter, have been modeled probabilistically, using a simple variant of equilibrium statistical mechanics. For reviews on such modeling see for instance [11–14]. Markov chain Monte Carlo simulation of our model suggests that dilatancy onset can be understood as a second order phase transition, a discontinuity in a second derivative of the appropriate free energy.

2 The Model

Our "granular hard cubes" model is a granular variant of the classical hard cubes model [15] of equilibrium statistical mechanics, the latter being a simplification of the classical hard sphere model in which the spheres are replaced by nonoverlapping, parallel cubes. So our model uses layered configurations of hard, parallel, unit cubic grains; see Fig. 1. To model the reaction to a change of strain we mimic the spherical caps that grains in one layer present to grains in neighboring layers by adding cubic "bumps" of width w to the top and bottom of our cubes; see Fig. 2. We use $w = 0.3$, a choice discussed below; see Fig. 3. As we will see below when we discuss dilatancy, these bumps use the third dimension to add a significant resistance to shear. In our model each grain must sit on exactly four other grains (except grains on the boundary of the configuration), and grains cannot overlap. We do not allow any grain to sit on the bump of another grain; thus, the grains appear on discrete vertical layers, so the distance in the direction of gravity (or z-direction) between the centers of grains on adjacent layers is equal to 1; see Fig. 4. There are n^2 grains in each layer, and n total layers, so there are $N = n^3$ total grains.

For boundary conditions we require that in a given configuration the centers of the grains on the boundary in a single layer all lie on the edges of a rhombus with angle of strain α and area L^2, where $\alpha = 0$ represents a square (see Fig. 2a). Thus, our configurations have boundaries which are essentially cylinders on rhombic bases. The volume of a configuration is then defined as $V = nL^2$. To prevent grains from getting stuck between the boundary grains, we impose top-bottom periodic boundary conditions, and we remove the bumps from the grains nearest to the boundary and on the boundary. We restrict α to $\alpha \geq 0$ since the

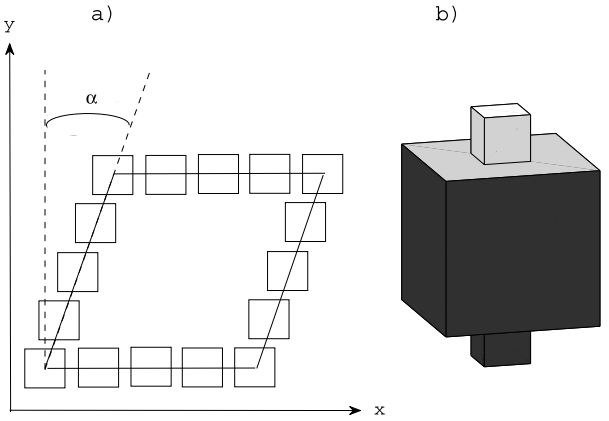

Fig. 2 (**a**) A view from above of a layer in a configuration (only boundary grains, and without their bumps), with a definition of the strain angle α; (**b**) A cubic grain, with bumps on top and bottom faces

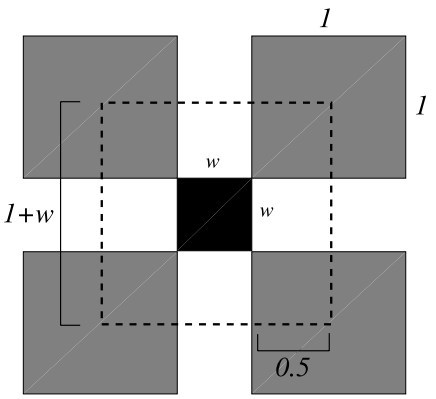

Fig. 3 A *horizontal cross-section* of the closest packing possible of maximally regular grains, with *the small black square* representing a bump. By partitioning along the *dotted lines*, one can calculate the particle density of the configuration, $\phi = (1 + w)^{-2}$

shapes of configurations corresponding to angles α of opposite sign are merely rotations of one another. (It is more complicated, and unnecessary, to model the effect of shear stress on the two representations of the same shape.) A configuration C is represented by the centers of all the grains in C, i.e. $C \in (\mathbb{R}^2 \times \mathbb{Z})^N$ (the grains are given an arbitrary fixed labeling, and the center of a grain is the center of the unit cube comprising the grain). A single grain g in C is represented by its center, $(x_g, y_g, z_g) \in \mathbb{R}^2 \times \mathbb{Z}$. For simplicity we require one of the grain centers to be at the origin, and all of the grain centers to be in the octant $x \geq 0$, $y \geq 0$, $z \geq 0$.

We use the following "volume/strain" ensemble. (Related ensembles have been used previously in granular modeling—see for instance [16, 17]—as well as modeling thermal systems—see for instance [18, 19].) Our ensemble, instead of fixing volume and strain, uses Lagrange multipliers p and f to control average volume and strain. The Lagrange multipliers enter into the maximization of entropy in the usual way. (In the literature $1/p$ and $1/f$ are sometimes called compactivity and angoricity.) In other words the states of the model, which, in the general approach of Edwards [9] are probability densities of configurations of grains, optimize the free energy

$$F(p, f) := S - pV + f\alpha V, \tag{1}$$

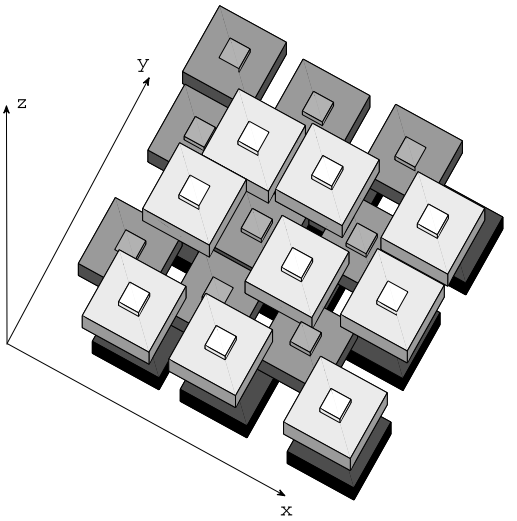

Fig. 4 An arrangement of grains, viewed from above

where S is the entropy, V is the volume in physical space, and $\alpha \geq 0$ represents the angle of strain (see Fig. 2a). The ensemble partition function is

$$Z_{p,f} = \int_0^\infty \int_0^\infty \left(\int_{V,\alpha} dC \right) \exp(-pV + f\alpha V)\, dV\, d\alpha, \tag{2}$$

where $\int_{V,\alpha} dC$ represents integration over the space of allowed configurations at fixed α and V, and $\ln(\int_{V,\alpha} dC)$ is the entropy $S = S(V, \alpha)$. Consider the change of coordinates $\psi_{V,\alpha}$ which maps configurations C at fixed V and α into $\Omega = ([0,1]^2 \times \{0, 1/n, 2/n, \ldots, 1\})^N$ such that $\psi_{V,\alpha}$ maps each grain center (x, y, z) to $(L^{-1}(x - \tan(\alpha)y), L^{-1}y, n^{-1}z)$. It is easy to see that this map has Jacobian equal to V^{-N}. Thus, using the new coordinates one can rewrite the partition function as

$$Z_{p,f} = \int_0^\infty \int_0^\infty \int_\Omega \Phi(\psi_{V,\alpha}^{-1}(Q))\, V^N \exp(-pV + f\alpha V)\, dQ\, dV\, d\alpha, \tag{3}$$

where $\Phi(C) = 1$ if C corresponds to a configuration which satisfies the conditions of the model, and $\Phi(C) = 0$ otherwise. The probability density of a configuration with volume V and strain angle α is therefore

$$m_{p,f}(C) = V^N \exp(-pV + f\alpha V)/Z_{p,f}. \tag{4}$$

Our model uses cubes instead of the more traditional spheres. Cubes are preferable here as they allow one to automatically maintain the contacts necessary to support grains 'under gravity' even while straining the system, a big advantage in the simulation. Another natural question is whether we can correctly model the response in density to shear stress when we only consider (configurational) states which are regular in the sense that the network of contacts in the system forms the same graph structure as a face centered cubic crystal.

It would be preferable to allow more general states, but this is very difficult in practice. And although such regular states may give misleading *quantitative* results for the response to shear, we expect to obtain the correct *qualitative* results, which is our only goal. In particular, the quantitative results we obtain are not meant to accurately represent real materials.

We show next why our model exhibits dilatancy onset: the separation of a high density regime of states, in which the material expands under infinitesimal shear, from a low density regime, in which it contracts under infinitesimal shear [1]. (The more interesting question, however, and the main focus of this paper, is whether the model predicts that the transition through dilatancy onset is singular in the parameter p.)

From the probability density of (4) it follows that if $f = 0$ then the state of lowest possible particle density, called random loose packing, occurs at $p = 0$ [20] and some strain $\alpha = \alpha_0$. (For this argument the value of α_0 is irrelevant.) At sufficiently low p and infinitesimal increase of f from 0, which should correspond to an infinitesimal shear stress, the density has no way to change except to increase. So at sufficiently low density there is a regime in which the system contracts under infinitesimal shear stress.

On the other hand, at least since Reynolds [2] one understands the expansion of (dense) granular matter under shear, which he termed dilatancy, in geometric terms, as the need for parallel layers of spheres to get out of each others' way under a strain deforming the layers, by separating and/or by thinning within the layers. For our grains, with bumps mimicking spherical caps, this thinning phenomenon should still be present. That is, for a sufficiently dense configuration, neighboring layers should "feel" each others' bumps, so that under an infinitesimal shear stress the layers should then spread out, producing a dilatancy effect. Note that, among optimally symmetric configurations (where the particle centers on each layer form a square lattice), at particle density $\phi_d := (1 + w)^{-2}$ the bumps on a given layer will touch the grains on the layer above. We interpret ϕ_d as a (rough) estimate of the minimal particle density required for dilatancy; see Fig. 3. In our simulations we use $w = 0.3$, and so $\phi_d \approx 0.59$. The qualitative dilatancy effect is not sensitive to the precise value of w, though the value ϕ_d is. To understand the choice of w consider the following. For cubes without bumps at zero pressure, a free volume estimate shows that the average particle density should be $9/16$. At this density, neighboring cubes in perfectly regular configurations of cubes will be separated by a distance of $1/3$, and so for such configurations adding a bump of width $w \leq 1/3$ will not create any overlap. We chose w slightly less than $1/3$, so that the cubes would not feel the bumps at low pressure, and also so that very high pressures weren't necessary to see the dilatancy effect.

So the bumps, together with the universal behavior at low p or density, explain the existence of dilatancy onset. The main question then is: as density is varied, does the transition through the dilatancy onset proceed in a smooth or in a singular manner? We will show there is an unambiguous second order phase transition at dilatancy onset, at density near $\phi_d = 0.59$. This suggests, by analogy with matter in thermal equilibrium, that the material in the two regimes differs in other characteristics as well, for instance it would be expected that the yield force would behave differently in the two regimes. In [8] the yield force is measured as a function of density, and a second order phase transition is found at a density roughly 0.598. Dilatancy onset was not carefully measured because of the experimental setup, but in other experiments has approximately coincided with the yield transition. Our result suggests the yield transition and dilatancy onset are simply different manifestations of the same phenomenon.

3 The Simulation, and Results

Each simulation of N particles begins with $\alpha = 0$ and $V > N/\phi_d$. The basic Monte Carlo step is as follows. Let $C(k)$ be the configuration at the kth step of the Monte Carlo chain, where $C(k)$ has volume V and strain α. For each grain g in $C(k)$ let (x_g, y_g, z_g) be the coordinates of the center of g. We allow three types of move, each of which produces a trial configuration C'. In the first type a single particle moves locally, in the second type the configuration changes volume, and in the third type the configuration changes shape.

The first type of move is attempted with probability $1 - 1/N$. For this type of move we choose a random non-boundary grain g in $C(k)$, and obtain C' by replacing g with a grain centered at $(x_g + \beta\gamma, y_g + (1-\beta)\psi, z_g)$. Here β is a Bernoulli random variable, i.e. $\beta = 0$ or 1 each with probability $1/2$, and γ and ψ are random variables uniformly distributed in the largest intervals (a_1, a_2) and (b_1, b_2) containing zero such that, for all $a \in (a_1, a_2)$ and $b \in (b_1, b_2)$, replacing g with a grain centered at $(x_g + a, y_g, z_g)$ or $(x_g, y_g + b, z_g)$ does not create overlap of grains. Such moves will produce configurations satisfying the conditions of the model, and are accepted with probability 1.

The second and third types of move are each attempted with probability $1/(2N)$. Let η, ν be random variables distributed uniformly in $(-1, 1)$, and fix (small) positive real parameters ϵ and δ. For the second type of move, we obtain C' by replacing (x_g, y_g, z_g) by $(\lambda x_g, \lambda y_g, z_g)$ for each grain g in $C(k)$, where $\lambda = (V + \eta\epsilon)^{1/2}/V^{1/2}$. For the third type of move, we obtain C' by replacing (x_g, y_g, z_g) by $(x_g + \nu\delta y_g, y_g, z_g)$ for each grain g in $C(k)$.

By construction the probability density of proposing a move $C \to C'$ is the same as the probability density of proposing a move $C' \to C$. To preserve detailed balance, the acceptance probability for the latter two types of moves is therefore

$$p = \min(1,\ \Phi(C')(V'/V)^N e^{-p(V'-V)+f(\alpha' V' - \alpha V)}), \tag{5}$$

with V' the volume of C' and α' the strain angle of C', and where, as above, $\Phi(C') = 1$ if C satisfies the conditions of the model and $\Phi(C') = 0$ otherwise. So for moves of the second and third type, we set $C(k+1) = C'$ with probability p, and $C(k+1) = C(k)$ with probability $1 - p$. Thus, the Monte Carlo steps are chosen so that the stationary distribution of the Markov chain has the desired limiting probability distribution (4).

In our simulations, we want to measure how the average of the density $\phi = N/V$ changes as f varies near $f = 0$. (For convenience we do not include the bumps in the calculation of ϕ, but since particle number N is fixed in our simulation, the "true" volume fraction is just a constant multiple of ϕ.) That is, we want to estimate the derivative

$$D(p) := \left.\frac{\partial \langle\phi\rangle_{p,f}}{\partial f}\right|_{f=0} \tag{6}$$

of the average $\langle\phi\rangle_{p,f}$ of ϕ as a function of p. So $D(p) < 0$ (resp. $D(p) > 0$) represents volume expansion (resp. contraction) under infinitesimal strain, which is directly relevant to our study of dilatancy onset.

From the definition of $m_{p,f}$ in (4) we have

$$\langle\phi\rangle_{p,f} = \frac{1}{Z_{p,f}} \int_0^\infty \int_0^\infty \int_\Omega \frac{N}{V} \Phi(\psi_{V,\alpha}^{-1}(Q))\, V^N \exp(-pV + f\alpha V)\, dQ\, dV\, d\alpha, \quad (7)$$

from which it follows by differentiation that

$$D(p) = \left.\frac{\partial\langle\phi\rangle_{p,f}}{\partial f}\right|_{f=0} = N\langle\alpha\rangle_{p,0} - [\langle\phi\rangle_{p,0}][\langle V\alpha\rangle_{p,0}]. \quad (8)$$

Thus, to estimate $D(p)$ from our simulations we set $f = 0$ and calculate the sample averages of $N\alpha$, ϕ, and $V\alpha$. With the free energy $F(p, f) = S - pV + f\alpha V = \ln(Z_{p,f})$, which is the quantity minimized by the state $m_{p,f}$, one can see from (1), (3) and (7) that

$$\frac{\langle\phi\rangle_{p,0}^2}{N} \frac{\partial}{\partial f}\left(\frac{\partial F(p, f)}{\partial p}\right)\bigg|_{f=0} = \frac{\langle\phi\rangle_{p,0}^2}{N} \frac{\partial}{\partial f}\left(\frac{\partial \ln(Z_{p,f})}{\partial p}\right)\bigg|_{f=0} = D(p), \quad (9)$$

and so the function $D(p)$, as a second derivative of the free energy, is a quantity for which a discontinuity might reasonably be described as a second order phase transition.

We investigate systems of $N = 8^3 = 512$, $10^3 = 1000$, $12^3 = 1728$, $14^3 = 2744$ and $16^3 = 4096$ grains at $p_1 < \cdots < p_k$, where the p values chosen are different for each size system. In the simulations we begin at low p_1, and then slowly increase p until just after the derivative $D(p)$ falls sharply below zero, roughly corresponding to p_k. (For pressures significantly greater than p_k, the simulations become prohibitively slow.) The last configuration in the simulation of p_i is used as the starting configuration of the simulation of p_{i+1}. We use the standard biased autocorrelation function to determine a "mixing time", measured as the number of Monte Carlo steps required before the autocorrelation first crosses zero, and we run our simulations long enough so that the simulation of each p_i contains on average at least 20 mixing times. Then we run 200 independent copies of each simulation to obtain the averages $\langle\alpha\rangle_{p,0}$, $\langle\phi\rangle_{p,0}$, and $\langle V\alpha\rangle_{p,0}$. With these averages we compute $D(p)$ from (8). (We also ran some of our simulations much longer, with fewer copies and p values, and noted agreement with the already-obtained data on $D(p)$.) Then, for error bars on $D(p)$, we repeat the entire experiment 8 times and use the Student's t-distribution.

Our simulations suggest that $D(p)$ develops a discontinuity as the system size increases (see Fig. 5). Changing variables we find that D, as a function of $\langle\phi\rangle_{p,0}$, develops a discontinuity. We note that the ϕ-values where $D(p)$ drops sharply below zero are relatively close to the volume fraction $\phi_d \approx 0.59$ noted in the introduction. However because the sharp drop in $D(p)$ moves significantly with system size it is hard to pinpoint a precise transition point. We plot $\langle\phi\rangle_{p,0}$ against p in Fig. 6b and D against $\langle\phi\rangle_{p,0}$ in Fig. 6a.

Note that for $p \leq 1$, $D(p)$ exhibits regular behavior in which $D(p)$ is roughly constant, $D(p) = \eta \approx 0.001$. Then for $1 < p < 2$, $D(p)$ has some oscillation which is characteristic to the system size. Then for $p \geq 2$, $D(p)$ steadily increases to a peak, then sharply decreases through zero. We believe that $D(p)$ is discontinuous in the limit of infinite system size, but the rate of change of $D(p)$ is so large it is difficult to measure its variation with system size. Instead we consider two measures of the interval R in which the discontinuity is developing, and then note that R gets smaller and smaller as system size increases.

We expect that the oscillation observed in $D(p)$ in the interval $1 < p < 2$ is caused by finite-size effects, so that it disappears in the limit $N \to \infty$. Furthermore we expect the critical p_c to fall at either the end or the beginning of the oscillation region. These

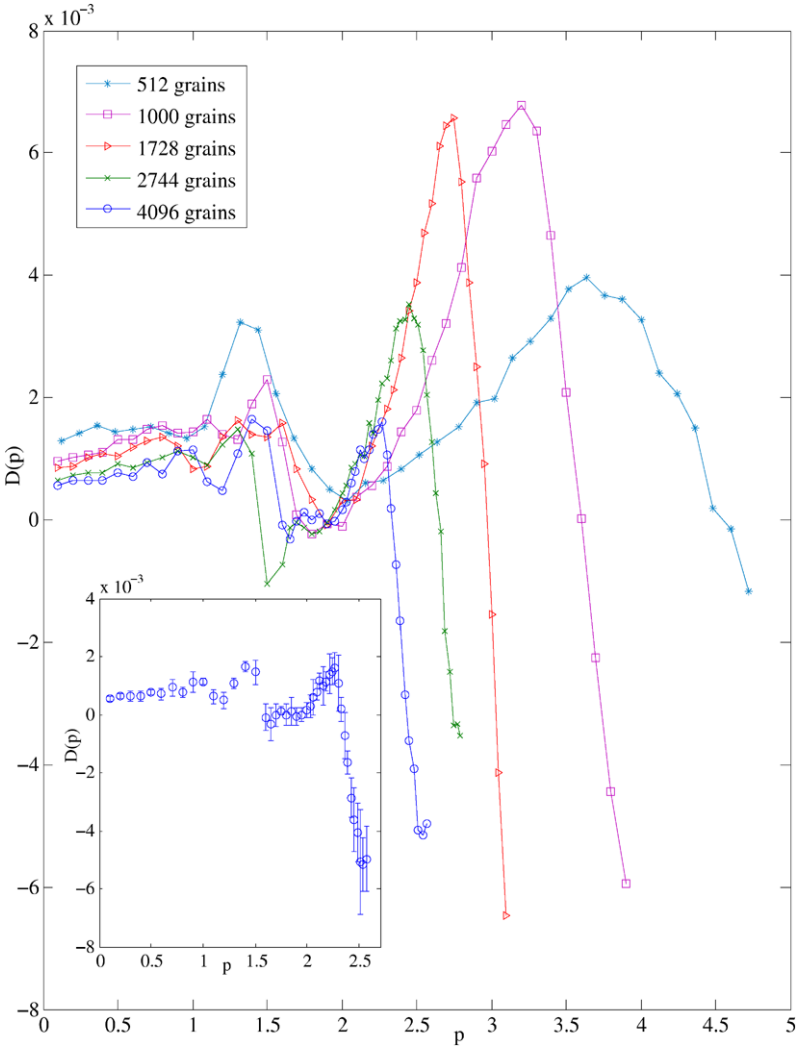

Fig. 5 The graph of $D(p) = \frac{\partial \langle \phi \rangle_{p,f}}{\partial f}|_{f=0}$, which measures the response in average density, $\langle \phi \rangle_{p,f}$, to change of strain. The *insert* gives error bars on the system with 4096 grains

two possibilities underlie, respectively, our measurements R_1 and R_2, defined below. Let η be the average value of $D(p)$ over $p \leq 1$. The left endpoint of R_1 is the smallest value of p where $p > 2$ and $D(p) \approx \eta$, and the right endpoint of R_1 is the value of p where $p > 2$ and $D(p) \approx 0$. The widths of R_1 are approximately 1.75 ± 0.05, 1.15 ± 0.05, 0.75 ± 0.05, 0.50 ± 0.05, and 0.30 ± 0.05 for systems of $N = 8^3$, 10^3, 12^3, 14^3 and 16^3 grains, respectively. On the other hand, the left endpoint of R_2 is defined as the smallest value of p such that $D(p)$ differs significantly from η, while the right endpoint of R_2 is the same as the right endpoint of R_1. We estimate that the widths of R_2 are approximately 3.55 ± 0.05, 1.55 ± 0.05, 1.25 ± 0.15, 1.15 ± 0.05, and 1.00 ± 0.05 for systems of $N = 8^3$, 10^3, 12^3, 14^3 and 16^3 grains, respectively.

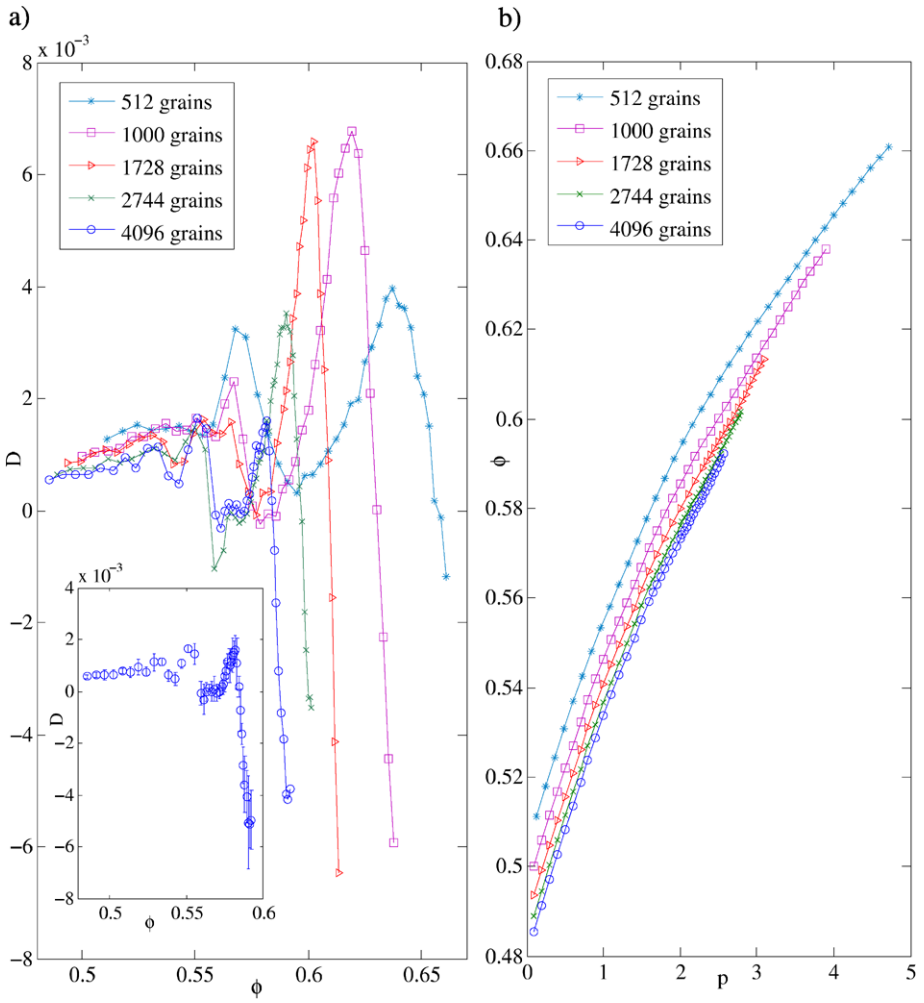

Fig. 6 (**a**) $D(p)$, our measure of the response of density to change of strain, as a function of the average density, ϕ; (**b**) The average density, ϕ, as a function of p

In either case, based on the decreasing sizes of the intervals R_1 and R_2, we believe that the jump from $D(p) \approx \eta$ to $D(p) \ll 0$ occurs over an interval which is vanishing in the infinite volume limit, which, given the relation between $D(p)$ and the free energy $F(p, f)$ in (9), is reasonably termed a second order phase transition. And as noted in the introduction, there is experimental evidence for this interpretation in [8].

4 Conclusion

We have analyzed a model of granular matter using an Edwards ensemble [11–14], the purpose being to understand the yield phase transition found in [8]. The transition in [8] occurs at approximately the same volume fraction, about 0.6, as dilatancy onset [1], but

corresponds to a different response of the material, a penetration force instead of a shear. Our granular model shows that shearing could produce a sharp phase transition at dilatancy onset, defined as the boundary between the volume fractions which expand under shear and those which contract under shear. As the two physical phenomena, the yield transition and dilatancy onset, both occur at volume fractions near 0.6, we argue that they coincide, in the sense that they simply represent responses of two phases of granular matter to different stimuli.

We also note that the behavior of granular matter at the random close packing density, about 0.64, has been interpreted in [21, 22] as the freezing point of a first order phase transition in which the high density regime is an ordered phase. Together with our results here, this means that the usual freezing transition of equilibrium fluids, at which the material acquires the solid features of an ordered (typically crystalline) internal structure as well as a strong resistance to shear, seems to be split into two stages in granular materials, with significant resistance to shear occurring at dilatancy onset at density about 0.6 [1] and the ordered internal structure occurring at the random close packing density of about 0.64 [23].

A direct test of whether dilatancy onset defines a sharp phase transition poses some experimental difficulty. The statistical approach seems to require that repeated preparations of granular samples be able to sample the full granular phase space. This seems to be justified for the fluidization/sedimentation method of [8], and the tapping method of [7]. A test would therefore require a way to combine shearing with one of these preparation protocols. It should be possible to perform a tapping protocol in a shear cell, but tapping does not ordinarily produce samples at volume fractions below 0.6, making it hard to see dilatancy onset. And while fluidization/sedimentation can prepare samples in the desired range of volume fractions, this protocol is hard to perform in a shear cell.

On the theoretical side, our result helps to firm up the phase diagram of granular matter. There was already experimental [24] and theoretical [21, 22] support for a phase transition at random close packing, which is at volume fraction 0.64. Our result adds theoretical support to the experimental evidence of [8] for a phase transition at volume fraction 0.6.

The statistical modeling of granular matter using ensembles of Edwards' type is, presumably, justifiable only for certain preparation protocols, such as the fluidization/sedimentation and tapping noted above. We hope that the growing evidence of interesting structure in the state space of granular matter will help motivate further experimental development to investigate these states, the analogue of the states of matter in thermal equilibrium.

Acknowledgements It is a pleasure to acknowledge useful discussions with Hans C. Andersen, Paul Chaikin and Matthias Schröter. Research of C. Radin supported in part by NSF Grant DMS-0700120.

References

1. Rao, K.K., Nott, P.R.: An Introduction to Granular Flow. Cambridge University Press, Cambridge (2008)
2. Reynolds, O.: Phil. Mag. Series 5 **20**, 469 (1885)
3. Aharonov, E., Sparks, D.: Phys. Rev. E **60**, 6890 (1999)
4. Piccioni, M., Loreto, V., Roux, S.: Phys. Rev. E **61**, 2813 (2000)
5. Tillemans, H.-J., Herrmann, J.: Physica A **217**, 261 (1995)
6. Coniglio, A., Herrmann, H.J.: Physica A **225**, 1 (1996)
7. Nowak, E.R., Knight, J.B., Ben-Naim, E., Jaeger, H.M., Nagel, S.R.: Phys. Rev. E **57**, 1971 (1998)
8. Schröter, M., Nägle, S., Radin, C., Swinney, H.L.: Europhys. Lett. **78**, 44004 (2007)
9. Edwards, S.F., Oakeshott, R.B.S.: Physica A **157**, 1080 (1989)
10. de Gennes, P.-G.: Scaling Concepts in Polymer Physics. Cornell University Press, Ithaca (1979)
11. Barrat, A., Kurchan, J., Loreto, V., Sellitto, M.: Phys. Rev. Lett. **85**, 5034 (2000)

12. Chakraborty, B.: Soft Matter **6**, 2884 (2010)
13. Edwards, S.F., Grinev, D.V.: Adv. Phys. **51**, 1669 (2002)
14. Herrmann, H.J.: Physica A **263**, 51 (1999)
15. Hoover, W.G., Hoover, C.G., Bannerman, M.N.: J. Stat. Phys. **136**, 715 (2009)
16. Bi, D., Chakraborty, B.: Philos. Trans. R. Soc. Lond. **367**, 5073 (2009)
17. Blumenfeld, R., Edwards, S.F.: J. Phys. Chem. B **113**, 3981 (2009)
18. Parrinello, M., Rahman, A.: J. Chem. Phys. **76**, 2662 (1982)
19. MacDonald, I.R.: Mol. Phys. **100**, 95 (2002)
20. Aristoff, D., Radin, C.: J. Stat. Phys. **135**, 1 (2009)
21. Radin, C.: J. Stat. Phys. **131**, 567 (2008)
22. Aristoff, D., Radin, C.: J. Math. Phys. **51**, 113302 (2010)
23. Scott, G.D., Kilgour, D.M.: Br. J. Appl. Phys. **2**, 863 (1969)
24. Scott, G.D., Charlesworth, A.M., Mak, M.K.: J. Chem. Phys. **40**, 611 (1964)